Inorg. Chem. **2009**, *48*, 2136−2139

Thermochromic Phase Transition on $CuMo_{0.9}W_{0.1}O_4$@SiO_2 Core−Shell Particles

M. Gaudon,* B. Basly, Y. Fauque, J. Majimel, and M. H. Delville*

Institut de Chimie de la Matière Condensée de Bordeaux, UPR 9048 CNRS 87 Avenue du Dr. Schweitzer, 33608 Pessac Cedex, France

Received October 27, 2008

The thermochromic phase transition of $CuMo_{1-x}W_xO_4$ oxide was delayed by the deposit of SiO_2 shells. The phase transition temperature was investigated by optical reflectivity versus temperature. The effect of the shell thickness on the transition temperature is established. The cyclability of the phenomenon is also discussed.

Introduction

A thermochromic substance changes its color when subjected to temperature variation in a certain range. Besides the materials based on organic molecules such as spiropyran and ethylene derivatives,[1] or liquid crystals,[2] widely applied as thermo-indicators and thermometers, there has been an increasing interest in applied research for the thermochromic properties of inorganic materials, as used in optical switching elements[3] and smart windows.[4,5]

However, very little attention has been paid to the thermochromism which takes place in the very few ceramics that are able to show this interesting phenomenon.[6,7] We have shown in recent studies that, at ambient pressure, $CuMo_{0.9}W_{0.1}O_4$ oxide changes its color because it crystallizes in two polymorphs, that is, a high-temperature−low-pressure form (α form with green coloration) and a low-temperature−high-pressure one (γ form with reddish brown coloration).[8−10] The γ→α phase transition occurs by warming at 85 °C, and the reverse one occurs by cooling at about −20 °C. For some of the desired industrial applications, such a thermochromism should occur over 150 °C and be reversible above room temperature; that is, the phase transition temperatures should be increased. The first-order phase transition between the two structures is associated with a variation of about 10% of the unit cell volume at the transition.[11] The first report on the stabilization of the γ-$CuMoO_4$ phase with tungsten doping was reported by Wiesmann et al.;[12] the first study on the optical properties of such compounds was made by Rodriguez et al.[13]

Silica coatings on core particles have proved to be efficient for modifying the core intrinsic properties. As examples, a size dependence of the melting temperature of silica-encapsulated gold nanoparticles[14] and a modification of the blocking temperatures (T_B) between the FePt and FePt@SiO_2 nanoparticles[15] have been observed.

In the present work, we show that it is possible to delay and therefore to control the transition temperatures by the deposit of SiO_2 shells around the γ-$CuMo_{0.9}W_{0.1}O_4$ cores. Indeed, one can imagine that constraints will take place because of the shell during the volume expansion associated with the γ→α phase transition. Hence, the high-pressure

* To whom correspondence should be addressed. E-mail: gaudon@icmcb-bordeaux.cnrs.fr (M.G.), delville@icmcb-bordeaux.cnrs.fr (M.H.D.).

(1) Day, J. H. *Chem. Rev.* **1963**, *63*, 65.
(2) See, for example, U.S. Patents 3 114 836 (1963) and 3 440 882 (1969).
(3) Vernardou, D.; Pemble, M. E.; Sheel, D. W. *Chem. Vap. Deposition* **2007**, *13*, 158.
(4) Kakiuchida, H.; Jin, P.; Okada, M.; Tazawa, M. *Jpn. J. Appl. Phys.* **2007**, *46*, 621.
(5) Piccirillo, C.; Binions, R.; Parkin, I. P. *Chem. Vap. Deposition* **2007**, *13*, 145.
(6) Lebedeva, N. N.; Arushanov, A. G.; Zeynally, Kh. A. *Physica B* **1989**, *154*, 209–213.
(7) Tang, G.; Yu, Y.; Chen, W.; Cao, Y. *Mater. Lett.* **2008**, *62*, 17–18.
(8) Gaudon, M.; Deniard, P.; Demourgues, A.; Thiry, A.-E.; Carbonera, C.; Le Nestour, A.; Largeteau, A.; Létard, J.-F.; Jobic, S. *Adv. Mater.* **2007**, *19*, 3517.
(9) Thiry, A. E.; Gaudon, M.; Payen, C.; Daro, N.; Létard, J.-F; Gorsse, S.; Deniard, P.; Rocquefelte, X.; Demourgues, A.; Whangbo, M.-H.; Jobic, S. *Chem. Mater.* **2008**, *20* (6), 2075.
(10) Gaudon, M.; Carbonera, C.; Thiry, A.-E.; Demourgues, A.; Deniard, P.; Payen, C.; Létard, J.-F.; Jobic, S. *Inorg. Chem.* **2007**, *46*, 10200.
(11) Ehrenberg, H.; Weitzel, H.; Paulus, H.; Wiesmann, M.; Wltschek, G.; Geselle, M.; Fuess, H. *J. Phys. Chem. Solids* **1997**, *58*, 153.
(12) Wiesmann, M.; Ehrenberg, H.; Miehe, G.; Peun, T.; Weitzel, H.; Fuess, H. *J. Solid State Chem.* **1997**, *132* (1), 88.
(13) Rodríguez, F.; Hernández, D.; Garcia-Jaca, J.; Ehrenberg, H.; Weitzel, H. *Phys. Rev. B: Condens. Matter Mater. Phys.* **2000**, *61* (24), 16497.
(14) Dick, K.; Dhanasekaran, T.; Zhang, Z.; Meisel, D. *J. Am. Chem. Soc.* **2002**, *124, 10*, 2312–2317.
(15) Aslam, M; Fu, L; Li, S.; Dravid Vinayak, P. *J. Colloid Interface Sci.* **2005**, *290*, 444.

10.1021/ic802057c CCC: $40.75
Published on Web 01/30/2009

(low-temperature) form should be stabilized, and the $\gamma \rightarrow \alpha$ transition temperature should be increased.

Experimental Section

The starting γ-$CuMo_{0.9}W_{0.1}O_4$ powder is produced by a conventional solid-state route at 700 °C under air followed by a mechanical grinding. The powder is then dispersed and coated with silica shells using a sol−gel process; the optimization of these two steps is discussed in the Results and Discussion section.[16,17]

To obtain the core−shell particles, the amount of tetraethylorthosilicate (TEOS) was determined according to eq 1:

$$V_{\mathrm{TEOS}} = N_{\mathrm{part}}[(\rho_{\mathrm{SiO_2}} M_{\mathrm{TEOS}})/(M_{\mathrm{SiO_2}} \rho_{\mathrm{TEOS}})] V_{\mathrm{SO_2}} \qquad (1)$$

with

$$N_{\mathrm{part}} = m_{\mathrm{CuMo_{0.9}W_{0.1}O_4}} / \left(4/3\pi R r^3 \rho_{\mathrm{CuMo_{0.9}W_{0.1}O_4}}\right)$$

and

$$V_{\mathrm{SiO_2}} = \left[4/3\pi(r + \mathrm{e_{shell}})^3 - 4/3\pi r^3\right]$$

where $\rho_{\mathrm{SiO_2}}$, $V_{\mathrm{SiO_2}}$, and $M_{\mathrm{SiO_2}}$ are the density volume and molecular weight of SiO_2 and ρ_{TEOS}, V_{TEOS}, and M_{TEOS} are the density volume and molecular weight of TEOS. N_{part} is the number of particles.

Additionally, the TEOS was added in several small fractions under mild stirring, one fraction a day, in order to limit the probability of its self-hydrolysis−condensation. Under such conditions, despite a rough control of the particles' surface area, secondary nucleation could essentially be prevented.[18] However, ammonia usually used for the Stöber process induced powder damage, as already mentioned. A set of organic amines $(CH_3)_nNH_{3-n}$ was checked in terms of long-term stability of the powder in such media, and the results showed that trimethyl amine was the best compromise for the encapsulation (no observed powder degradation during the time required for the coating).

Transmission electronic microscopy (TEM) was performed on TECNAI F20 equipment with a field emissive gun, operating at 200 kV and with a point resolution of 0.24 nm. Samples were prepared by dissolving a few milligrams of powder in ethanol or directly depositing one drop of the alkoxide solution on a Formvar/carbon copper grid.

Visible spectra in the 400−800 nm range between room temperature and 200 °C are recorded on a setup equipped with a photomultiplicator fiber. In both cases, the white light source was a halogen lamp and the heating/cooling rate was settled at 10 K min^{-1} and controlled with a standard tubular furnace.

Results and Discussion

The control of encapsulation by a silica shell is easier to perform when a low polydispersity of the particles can be achieved, which was not the case for high-temperature synthesized material. The very high sensitivity of γ-$CuMo_{0.9}W_{0.1}O_4$ powder to acidic or basic media, leading respectively to a superficial amorphization (Figure S1, Supporting Information) or a partial dissolution (Figure S2, Supporting Information) of the oxide, prevented the use of strong electrostatic repulsions to ensure its dispersion. Attempts were therefore performed in alcoholic media (EtOH), which is the further reaction solvent for silica encapsulation. However, even after the powder suspensions were ultrasonicated, the granulometry curves still showed a bimodal distribution (Figure 1a).

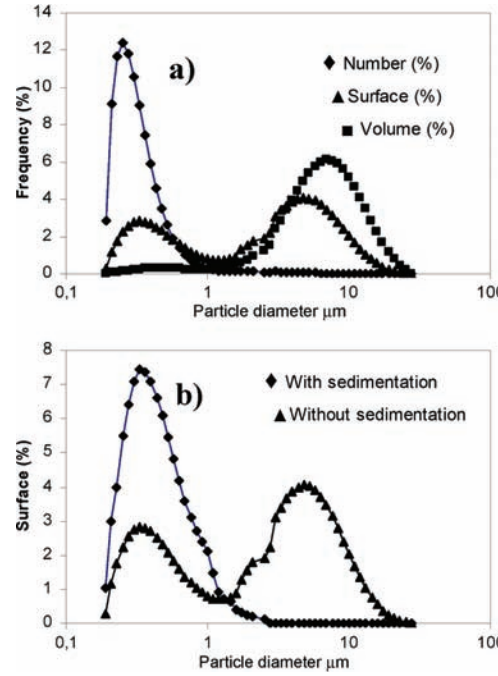

Figure 1. Granulometry distributions: (a) various presentations of the same dispersion, (b) comparison of this dispersion obtained with and without an additive gravimetric sorting.

Even if only a small minority of big agglomerates is still present (in number), their cumulated surface is of the same order as the surface of the dispersed particles of the first mode, and the volume of the powder is mainly constituted of the agglomerates. To solve this problem, granulometry sorting was performed: about 95% of the powder was let for sedimentation and was thrown away (Figure 1b). Thus, dispersion with a unique mode centered at about 0.2 μm could confidently be achieved. The synthesis of $CuMo_{0.9}W_{0.1}O_4$@SiO_2 particles is based on the growth of the silica shell through the TEOS hydrolysis/condensation process derived from the modified Stöber method.[16,17]

To coat the particles, the overall amount of added TEOS was set to comply with the desired silica shell thickness, according to eq 1 (see Experimental Section), and assuming an average size of 200 nm for the particles. The addition of TEOS in several fractions under mild stirring, in the presence of trimethyl amine over one to several days, limited the probability of nucleation of a secondary population.

TEM images show that both individual particles and agglomerates are coated. Very few silica spheres issued from secondary nucleation were also detected (Figure S3, Supporting Information). Nevertheless, there is an "average" effect which shows that the experimental thickness of the individual coated particles is directly correlated with the theoretical one, as shown in Figures 2 and 3, the theoretical thickness being calculated considering that all of the particles are spherical with about a 200 nm diameter.

(16) Stöber, W.; Fink, A.; Bohn, E. *J. Colloid Interface Sci.* **1968**, *26*, 62.
(17) Mornet, S.; Elissade, C.; Hornebeck, V.; Bidault, O.; Duguet, E.; Brisson, A.; Maglione, M. *Chem. Mater.* **2005**, *17*, 4530.
(18) Chen, S.-L.; Dong, P.; Yang, G.-H.; Yang, J.-J. *J. Colloid Interface Sci.* **1996**, *180*, 237.

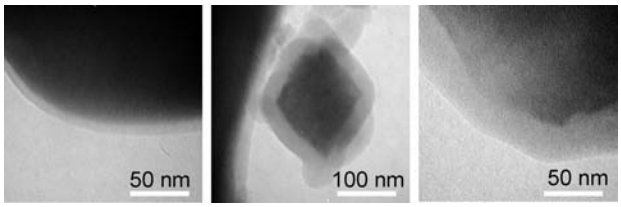

Figure 2. TEM pictures of the core@shell particles, with (a) 10 nm, (b) 30 nm, and (c) 50 nm silica shell thicknesses.

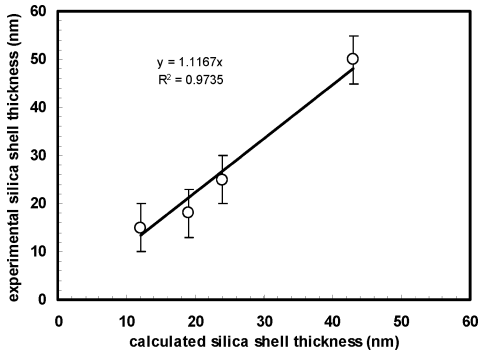

Figure 3. Variation of the experimental silica shell thickness of the $CuMo_{0.9}W_{0.1}O_4@SiO_2$ core−shell vs the theoretical one.

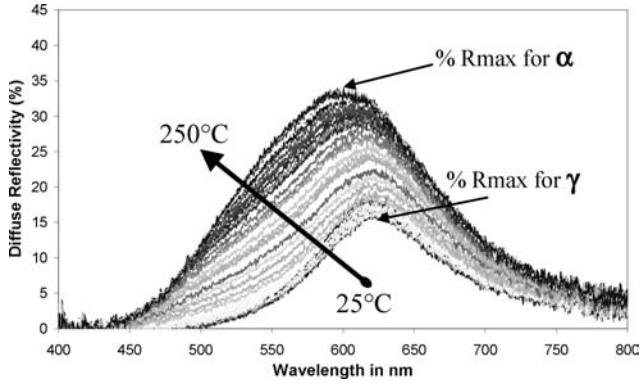

Figure 4. Variation of the diffuse reflectivity curve of one characteristic $CuMo_{0.9}W_{0.1}O_4@SiO_2$ core−shell vs temperature (silica thickness: 18 nm).

The slope in Figure 3, is characteristic of a slight overestimation of the overall particle surface area.

The effect of the SiO_2 coating on the transition temperatures between the two allotropic forms was observed by diffuse reflectivity measurement versus a temperature between room temperature and 300 °C.

Then, plotting the maximal reflectivity versus temperature gave S-type curves, which are reported in Figure 5; the optical contrasts between the low- and high-temperature forms are also determined.

The inflection point of the S curve (representing a mixture of 50% of each phase) can already be extracted. Nevertheless, for more accuracy, a correction in order to obtain standard S Boltzmann curves such as those reported in Figure 6 was performed. The latter represents how the transition width (here defined as the temperature width between the state with 10% α and 90% γ phase and that with 10% γ and 90% α phase) was also extracted.

The coating by a silica shell allows tuning of the transition temperature toward higher values. In the illustrated example (shell thickness of 18 nm), the transition temperature is nearly

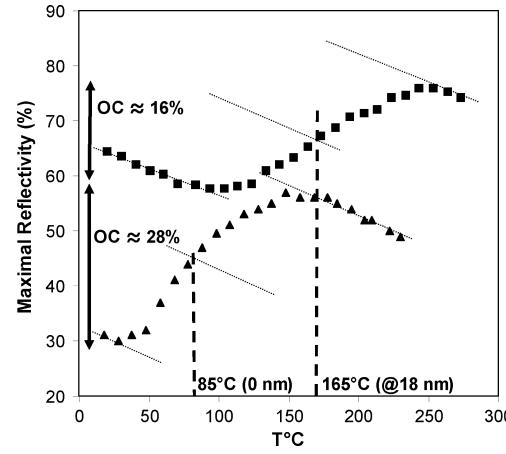

Figure 5. Maximal reflectivity of raw $CuMo_{0.9}W_{0.1}O_4$ and of $CuMo_{0.9}W_{0.1}O_4@SiO_2$ core−shell (18 nm thickness) vs temperature.

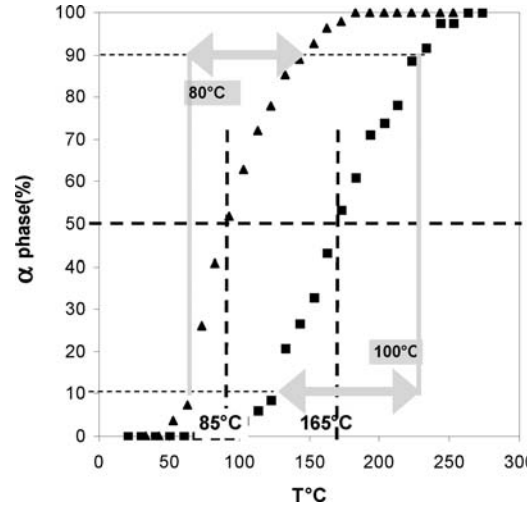

Figure 6. Variation of the α-form percentage vs temperature for γ-$CuMo_{0.9}W_{0.1}O_4$ (▲) and γ-$CuMo_{0.9}W_{0.1}O_4@SiO_2$ core−shell particles (18 nm) (■).

double that of the raw-core oxide (from 85 to 165 °C). Moreover, the transition width, which is around 80 °C for the raw-core oxide, goes up to 100 °C for the core@shell powder. The large transition width for the raw powder seems to be a consequence of the large granulometric distribution; the enlargement of this width with the shell deposit may hence be due, along the same lines, to a significant distribution of the core/shell size ratio.

The dependence of the transition temperature on the shell thickness for γ-$CuMo_{0.9}W_{0.1}O_4@SiO_2$ composites is compiled in Figure 7. The coating of the molybdates efficiently leads to an increase of the γ→α transition temperature with a width of transition that is rather constant (double arrow). The variation can be described by an asymptotic growth law, which is characteristic of an attenuation of the shell thickness effect on the transition temperature.

Eventually, the cyclability of the synthesized core@shell particle and, especially, the resistance of the shell during the γ→α transition were studied. TEM images and chemical cartographies obtained with coupled EDX analyses clearly show that the silica shell can severely crack during the transition because of the volume extension of the cores (see Figure 8). For a right perception of this phenomenon of the

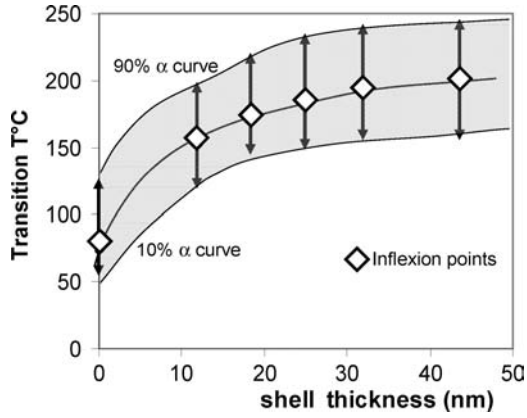

Figure 7. Evolution of the $\gamma \rightarrow \alpha$ transition temperature for various γ-$CuMo_{0.9}W_{0.1}O_4$@SiO_2 versus silica thickness.

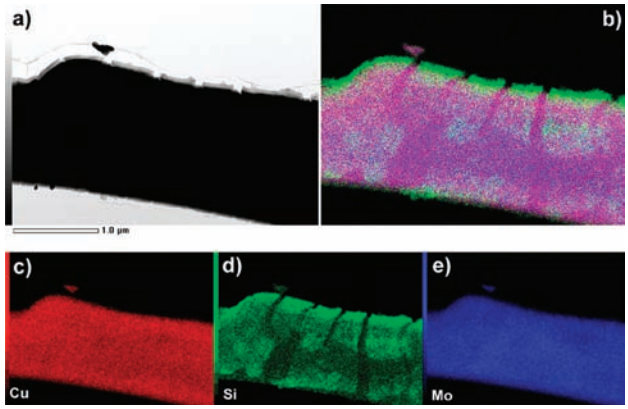

Figure 8. TEM images and chemical cartographies obtained with coupled EDX analyses for $CuMo_{0.9}W_{0.1}O_4$@SiO_2 core−shell obtained after the first $\gamma \rightarrow \alpha$ transition.

silica layer cracking, TEM micrographs, on a sample with a large core/shell diameter ratio and a 60 nm thickness silica layer, are presented.

A more accurate analysis shows that, actually, the shells crack when the core has overmicrometric dimensions. Consequently, during cycling (the materials were heated and cooled successively, one cycle being a complete $\gamma \rightarrow \alpha \rightarrow \gamma$ sequence), a significant deterioration of the shell takes place, with cracks appearing particularly during the first $\gamma \rightarrow \alpha$ transition. Therefore, during the following cycles, the shell's influence on the temperature was less efficient.

In Figure 9, the variation of the $\gamma \rightarrow \alpha$ transition (determined by reflectivity versus temperature) of an 18-nm-thick γ-$CuMo_{0.9}W_{0.1}O_4$@SiO_2 core−shell was compared in its first and third cycles.

It is clear that the deposited shell induces a large increase of the transition temperature from 85 °C for raw cores up to 165 °C for the first cycle; however, when successive cycles

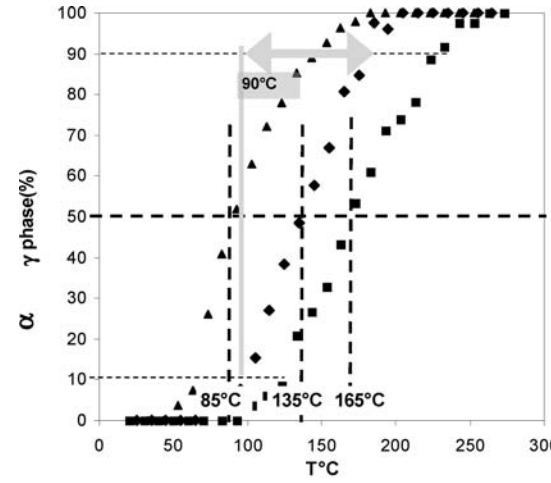

Figure 9. Variation of the α-form percentage vs temperature for γ-$CuMo_{0.9}W_{0.1}O_4$ (▲) and for γ-$CuMo_{0.9}W_{0.1}O_4$@SiO_2 core−shell, during the first cycle (■) and during the third cycle (♦).

are applied, a significant decrease of this transition temperature is observed. As an example, the third cycling already shows a temperature decrease down to 135 °C. Furthermore, the transition width also tends to diminish with cycling. From these results, we can infer that the silica shell deposited on the bigger core cracks during the first transition, leading to a first overestimation of the transition temperature of the overall powder, which tends to an equilibrium value after a couple of cycles.

To conclude, it was clearly shown here that it is possible to increase a first-order phase transition by coating the material with a silica shell. Here, constraints occurring during the transition are thus enhanced because the shell opposes a resistance to the high-volume dilatation associated with the phase transition. Hence, the high-pressure−low-temperature form is stabilized and the phase transition temperature is increased. It is possible to tune the transition temperature within a relatively large range through a shell thickness control. Beyond a critical ratio of the core diameter/shell thickness, the shell can crack during the first transition, which exhibits a strong effect only on the first transition cycle (80 °C increase instead of 50 °C for the following ones for an 18 nm shell thickness). Nevertheless, even if smaller, this shift of the transition temperature with such a small thickness of silica, could be improved for bigger ones and find new potential applications.

Supporting Information Available: Figures S1, S2, and S3. This material is available free of charge via the Internet at http://pubs.acs.org.

IC802057C